

9-2005

# Electron-impact ionization of hydrogen and lithiumlike systems

M A. Uddin

*University of Rajshahi*

Abul Kalam fazlul Haque

*University of Rajshahi*

A K. Basak

*University of Rajshahi*

Khondkar R. Karim

*Illinois State University*

B C. Saha

*Florida Agricultural and Mechanical University*

Follow this and additional works at: <https://ir.library.illinoisstate.edu/fpphys>



Part of the [Atomic, Molecular and Optical Physics Commons](#)

---

## Recommended Citation

Uddin, M A.; Haque, Abul Kalam fazlul; Basak, A K.; Karim, Khondkar R.; and Saha, B C., "Electron-impact ionization of hydrogen and lithiumlike systems" (2005). *Faculty publications – Physics*. 26.

<https://ir.library.illinoisstate.edu/fpphys/26>

**Electron-impact ionization of hydrogen and lithiumlike systems**

M. A. Uddin,\* A. K. F. Haque, and A. K. Basak

*Department of Physics, University of Rajshahi, Rajshahi-6205, Bangladesh*

K. R. Karim

*Department of Physics, Illinois State University, Normal, Illinois 61790, USA*

B. C. Saha

*Department of Physics, Florida A & M University, Tallahassee, Florida 32307, USA*

(Received 21 June 2005; published 14 September 2005)

The electron impact single ionization cross sections on a number of targets with atomic number  $Z=1-92$  in the H and Li isoelectronic sequences are calculated using a modified version of the recently propounded relativistic improved binary-encounter dipole (MRIBED) model [M. A. Uddin *et al.*, Phys. Rev. A **70**, 032706 (2004); **71**, 032715 (2005)]. The modified RQIBED (MRIBED) model along with a  $Z$ -dependent factor in it is found remarkably successful in the applications to H- and Li-like systems and also valid for the ionization of a filled  $s$  orbit including the He-like targets.

DOI: [10.1103/PhysRevA.72.032715](https://doi.org/10.1103/PhysRevA.72.032715)

PACS number(s): 34.80.Dp

**I. INTRODUCTION**

Electron impact (EI) is the major mode of ionization processes in fusion plasmas, besides being of fundamental interest in the atomic structure and collision mechanisms. In particular, the knowledge of ionization cross sections has wide applications in astrophysics, plasma physics, radiation physics, mass spectrometry, semiconductor physics, etc.

Both experiments and quantum-mechanical calculations generate cross-section data for selected targets at some discrete energies. On the other hand, the fields of applications require at least 20%–30% accurate cross sections for a wide range of targets and energies. This need can be best served by simple-to-use models that can provide a fast generation of reasonably accurate cross sections for any target over a wide domain of energies. This situation leads the practitioners in the applied fields to prefer the simple analytic models rather than the quantal calculations as the latter are arduous and not easy for the rapid generation of cross sections.

Reviews of EI ionization and associated empirical models are provided in Refs. [1–3]. A compilation of selected experimental and theoretical data are given by Tawara and Kato [4]. Among the various models, those of Thomson [5], Lotz [6,7] and Gryzinski [8] have historical interest. Recently, the empirical models of Bernstam, Ralchenko, and Maron (BRY) [9] and Deutsch and Märk (DM) [10–17] and the binary-encounter-dipole (BED) model of Kim and Rudd [18] have enjoyed wide applications in their respective domains. In particular, the BED model has demonstrated reasonable successes in the description of the EI ionization of molecular targets [19–23]. However, the model has been applied to only a few one-electron atomic ions like He<sup>+</sup> and Li<sup>2+</sup> [18].

Uddin *et al.* [24] proposed the relativistic improved binary-encounter dipole (MRIBED) model with incorpora-

tion of ionic and relativistic ingredients into the structure of the simplified version of improved-binary-encounter-dipole (siBED) model of Huo [25] and applied with remarkable successes to the description of the EI ionization of He-like systems [24],  $K$ -shell [26] ionization, and Be-like targets [27]. All of these studies brought out the existence of a generic set of values of the two parameters of the MRIBED model, thereby indicating some relevance of these parameters to the electronic structure of the species. The constant values  $d_1=d_2=0.0$  have been found good for both the  $K$ -shell ionization and the ionization of Be-like targets, where only the  $s$  orbits remain filled. Although the experimental EI cross sections for the He-like systems have been described well using the parameter values  $d_1=0.0$  and  $d_2=0.05$  in [24], a reexamination indicates that all these experimental data can also be reproduced satisfactorily within 20%–30% using the  $d_1=d_2=0.0$  generic values. Thus all cases of ionization in the filled  $s$  orbit can be accounted for by these generic values.

It may be of interest to explore the MRIBED model to targets with an unfilled  $s$  subshell. Hydrogenlike and lithiumlike targets are of the simplest structure in this category and may serve as test cases for the aforesaid study of application of the MRIBED model to the EI ionization from the unfilled  $s$  subshell. In the course of our investigation, we could not find any generic set of values akin to these H- and Li-like targets. We then keep the values of the two parameters fixed at the  $d_1=d_2=0.0$  values for the  $s$  orbit and incorporate a  $Z$ -dependent factor following the procedure of Fontes *et al.* [28] for application to the  $s$ -orbit ionization. This choice makes the expression for  $G$  in Eq. (7) of [26] much simpler as compared to either the siBED [25] or MRIBED [24,26] model. The model so framed is, henceforth, referred to as the modified RQIBED (MRIBED) model.

We apply the MRIBED model to calculate the EI single ionization cross sections of He, Ne<sup>8+</sup>, and U<sup>90+</sup> from the helium isoelectronic sequence H, He<sup>+</sup>, Mo<sup>41+</sup>, Dy<sup>65+</sup>, and U<sup>91+</sup> from the hydrogenic isoelectronic sequence and of Li, N<sup>4+</sup>, Ti<sup>19+</sup>, V<sup>20+</sup>, Cr<sup>21+</sup>, Mn<sup>22+</sup>, Fe<sup>23+</sup>, and U<sup>89+</sup> from the lithium

\*Electronic address: uddinmda@yahoo.com

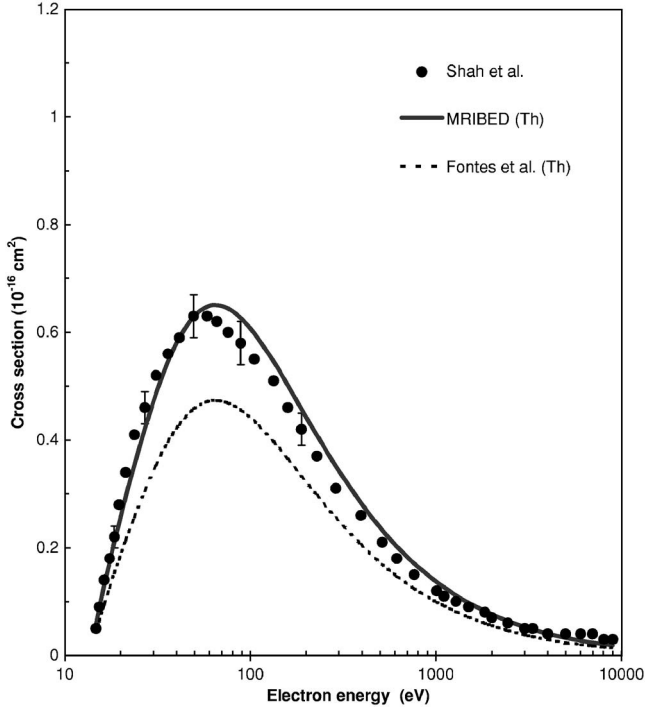


FIG. 1. The calculated EI ionization cross sections of H using the Z-dependent factor  $F_F(Z)$  of [28] (dashed curve) and the proposed  $F(Z)$  factor (solid curve) are compared with the experimental data in solid circles from Shah *et al.* [42].

isoelectronic sequence. The prediction from the MRIBED model is compared with the available experimental data, the calculations of BRY [9], and the modified Hombourger empirical (MHEMP) [29] models and other theoretical results. The theoretical methods used for comparison are the distorted-wave Born approximation (DWBA) [30,31], relativistic DWBA (RDWBA) [32], convergent-closed-coupling (CCC) approximation [33], relativistic two-potential distorted-wave (TPDW01) approximation [34], Coulomb-Born (CB) approximation [35], the analytic fit formula of Fontes *et al.* to the relativistic DWBA (FRDWBA) [36], and the assessed data of Bell *et al.* [37].

The paper is organized as follows. The MRIBED model is sketched in Sec. II. In Sec. III, we first revisit the EI ionization on He-like targets and then discuss the MRIBED results for the H- and Li-like systems in comparison with the available experimental cross sections and other theoretical findings. Section IV is devoted to the discussion of the results and the conclusions arrived at.

## II. OUTLINE OF THE MRIBED MODEL

In the MRIBED model with both its parameters set to  $d_1=d_2=0.0$ , the expression for the EI ionization cross section, following [26,27], can be obtained as

$$\sigma_{MRIBED} = \sigma_{Mott}^R + \sigma_{Born}^R, \quad (1)$$

where

$$\sigma_{Mott}^R = S^R H, \quad (2)$$

$$\sigma_{Born}^R = F^R G, \quad (3)$$

$$S^R = \frac{4\pi N_0 \alpha^2}{\beta_t^2 + (\beta_b^2 + \beta_a^2)/(q+1)}, \quad (4)$$

$$H = \left[ \frac{k_0^2 - \alpha_0^2}{k_0^2 \alpha_0^2} - \frac{\ln(k_0^2/\alpha_0^2)}{k_0^2 + \alpha_0^2} \right], \quad (5)$$

$$F^R = \frac{64\beta_a^3 N_0}{\alpha\beta_t^2}, \quad (6)$$

and

$$G = \int_0^{(k_0^2 - \alpha_0^2)/2} k_p (k_p^2 + \alpha_0^2)^2 dE_p \times \int_{K_{min}}^{K_{max}} \frac{1}{K[(K+k_p)^2 + \alpha_0^2]^3 [(K-k_p)^2 + \alpha_0^2]^3} dK. \quad (7)$$

In the above equations,  $T=k_0^2/2$  is the energy of the incident electron,  $U=k_b^2/2$  the kinetic energy of the bound electron,  $I=\alpha_0^2/2$  the binding energy of the target electron, and  $E_p=k_p^2/2$  the energy of the ejected electron with  $\alpha_0$  having the dimension of momentum in atomic units [25].  $\mathbf{K}=\mathbf{k}_0 - \mathbf{k}_1$  denotes the momentum transfer vector with  $\mathbf{k}_1$  representing the momentum of the electron after a collision in the atomic unit. The maximum and minimum values of  $K$  are given in [38].  $N_0$  is the number of electrons in the orbit considered, and  $q$  denotes the ionic charge of the target.

Using  $m$  as the mass of the electron,  $c$  as the velocity of light in the free space, and  $\alpha$  as the fine structure constant, the quantities  $\beta_t$ ,  $\beta_b$ , and  $\beta_a$  in Eqs. (4) and (6) are defined in terms of  $t'=k_0^2/(2mc^2)$ ,  $b'=k_b^2/(2mc^2)$ , and  $a'=k_0^2/(2mc^2)$ , respectively, as

$$\beta_t^2 = 1 - \frac{1}{(1+t')^2}, \quad (8)$$

$$\beta_b^2 = 1 - \frac{1}{(1+b')^2}, \quad (9)$$

and

$$\beta_a^2 = 1 - \frac{1}{(1+a')^2}. \quad (10)$$

In line with the form of the Z-dependent factor  $F_F(Z)$  of Fontes *et al.* [28] given by

$$F_F(Z) = [140 + (z/20)^{3.2}]/141, \quad (11)$$

the EI cross sections for an  $s$  orbit in the proposed MRIBED model can be evaluated by using

$$\sigma_{MRIBED} = (\sigma_{MRIBED})F(Z), \quad (12)$$

with

$$F(Z) = 1.0 \text{ for a filled } s \text{ orbit} \\ = 1 + mZ^n \text{ for an unfilled } s \text{ orbit}. \quad (13)$$

The reduced cross sections defined by

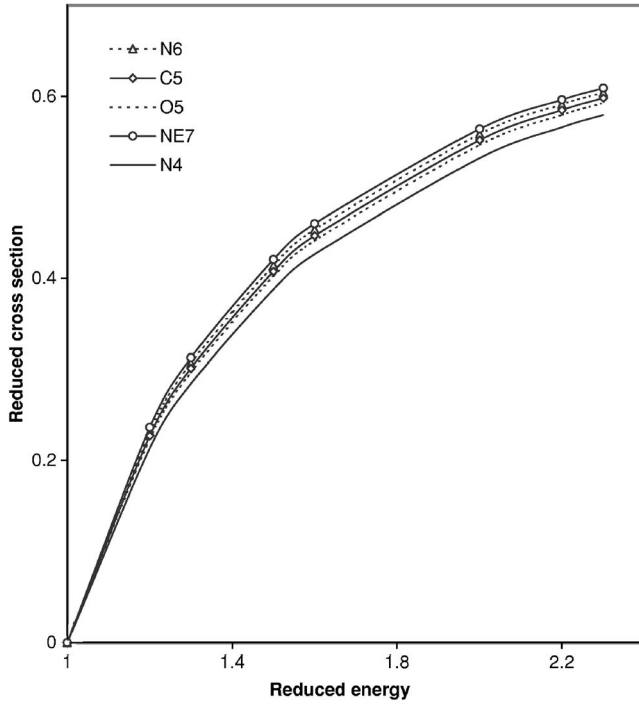


FIG. 2. The reduced cross sections of  $C^{5+}$ ,  $N^{4+,6+}$ ,  $O^{5+}$ , and  $Ne^{7+}$  as a function of reduced energy  $U=TI$ .

$$Q_U = \frac{I^2}{\pi a_0^2} \sigma_{MRIBED}, \quad (14)$$

with  $I$  in Rydberg units and  $a_0$  as the Bohr radius, are found to be independent of  $Z$  for the H and Li isoelectronic se-

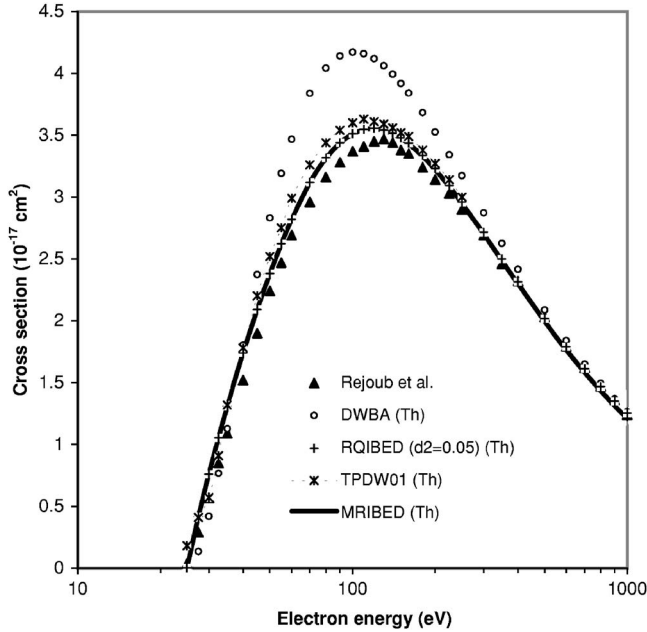


FIG. 3. The experimental EI ionization cross sections of H from Rejoub *et al.* [43] are compared with the MRIBED calculations (heavy solid curve), where  $d_2=0.0$ , and MRIBED predictions with  $d_2=0.05$  (pluses). The quantum-mechanical TPDW01 calculations of [34] are shown as the dotted curve with asterisks.

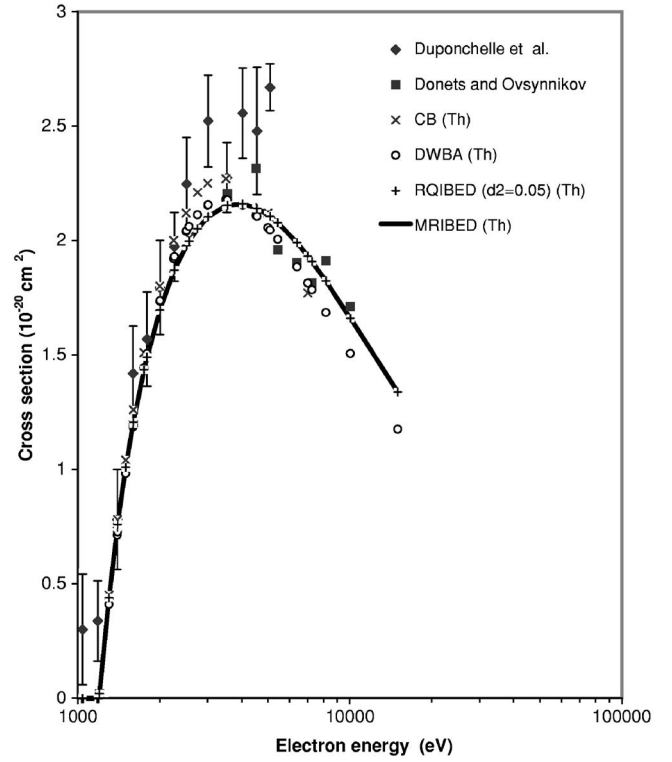


FIG. 4. Same as Fig. 3 for  $Ne^{8+}$  with the experimental data from Duponchelle *et al.* [44] and Donets and Ovsyannikov [45]. The DWBA and CB calculations are from [30] and [35], respectively.

quences for low incident energies. This finding encourages us to construct the  $\sigma_{MRIBED}$  in Eq. (12) following the procedure of Fontes *et al.* [28].

### III. RESULTS AND DISCUSSIONS

We have used published results for the ionization potentials given by Desclaux [39] for the neutral targets. The kinetic energies of all targets and ionization potentials of the ionic targets are calculated using the Dirac-Hartree-Fock code [40]. Using the 64-point Gauss-Legendre rule [41], the two-dimensional integrations over  $K$  and  $E_p$  [see Eq. (7)] are carried out numerically and the convergences are tested with increasing the Gaussian points. As mentioned earlier the parameters  $d_1$  and  $d_2$  are fixed at  $d_1=d_2=0.0$ . The values of the parameters  $m=0.365$  and  $n=0.050$  in Eq. (13) are determined from optimizing the overall fits of the MRIBED calculations with the experimental cross sections of all the targets in the H and Li isoelectronic sequences considered as well as  $Li^{2+}$ ,  $Be^+$ ,  $B^{2+}$ ,  $C^{3+,5+}$ ,  $N^{4+,6+}$ ,  $O^{5+,7+}$ ,  $Ne^{7+}$ ,  $Ar^{15+,17+}$ , and  $Fe^{23+}$  not included herein. Figure 1 compares the experimental cross sections for H with the calculated results using the factor  $F_F(Z)$  of [28] in Eq. (12) and the proposed factor  $F(Z)$  in the MRIBED model with  $m=0.365$  and  $n=0.050$ . An inclusion of a quadratic term in  $F(Z)$  does not improve the fits. Figure 2 displays the reduced cross sections  $Q_U$  in Eq. (14) for  $C^{5+}$ ,  $N^{4+,6+}$ ,  $O^{5+}$ , and  $Ne^{7+}$  and shows that the cross sections are almost  $Z$  independent at low energies. The calculated cross sections are summed over all the subshells.

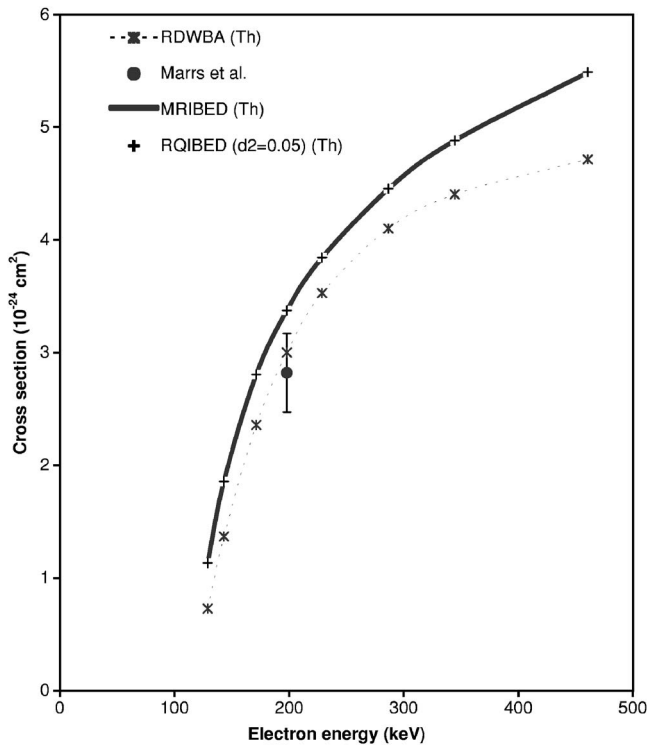


FIG. 5. Same as Fig. 3 for  $U^{90+}$ . The experimental data are from MARRS *et al.* [46]. The RDWBA calculations are from [32].

In Figs. 3–5 we compare the MRIBED predictions for the He,  $Ne^{8+}$  and  $U^{90+}$  with the experimental EI cross section data of Rejoub *et al.* [43], Duponchelle *et al.* [44], Donets and Ovsyannikov [45], and MARRS *et al.* [46] with the theoretical results from the MRIBED model using  $d_1=0.0$  and  $d_2=0.05$  [24], the present MRIBED model using  $F(Z)=1.0$ , the DWBA of Younger [30], TPDW01 [34], and RDWBA of [32]. Since the MRIBED calculations with  $F(Z)=1.0$  are equivalent to those of MRIBED with  $d_1=d_2=0.0$ , it is evident from the figures that the MRIBED results using  $d_2=0.05$  and those employing  $d_2=0.0$  with  $d_1=0.0$  in both cases are almost identical. Hence one can expect that the good performance of the MRIBED model on the He-like targets in [24] using  $d_1=0.0$  and  $d_2=0.05$  should also be achieved with  $d_1=d_2=0.0$ , the same optimum parameter values for the *K*-shell ionization [26] and ionization of the Be-like systems [27]. Thus in all the three cases with ionization from a filled *s* orbit, the appropriate values of the two parameters of the MRIBED model are  $d_1=d_2=0.0$ .

In Figs. 6–10 we compare the MRIBED predictions for the H,  $He^+$ ,  $Mo^{41+}$ ,  $Dy^{65+}$ , and  $U^{91+}$  targets in the H isoelectronic sequence with the experimental EI cross-section data of Shah *et al.* [42], Peart *et al.* [47], MARRS *et al.* [48], and Watanabe *et al.* [49]; the results from the MHEMP [29]; and the assessed data Bell *et al.* [37]. The other theoretical calculations used for comparison in these figures are TPDW01 of Kuo and Huang [34], RDWBA of Moores and Reed [32], and FRDWBA of Fontes *et al.* [36]. The RDWBA calculations include the Møller interaction [50] with consideration of exchange and interference effects. The DWBA calculations are the results from the fitting formula representing the

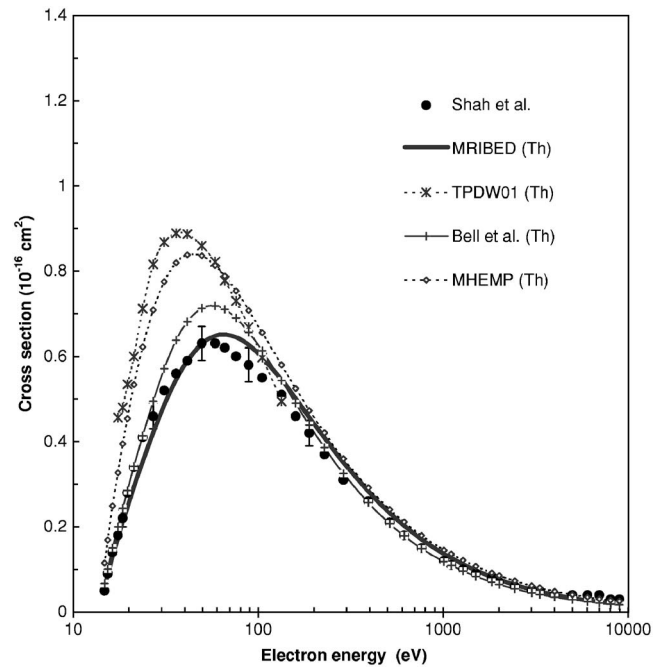


FIG. 6. The EI ionization cross sections of H versus electron energy. The experimental data are the solid circles from Shah *et al.* [42]. Calculated cross sections from the MRIBED and MHEMP models are shown as the heavy solid line and dotted curve with open diamonds, respectively. The TPDW01 calculations of [34] are shown as the dotted curve with asterisks. The solid curve with pluses represents the assessed data of [37].

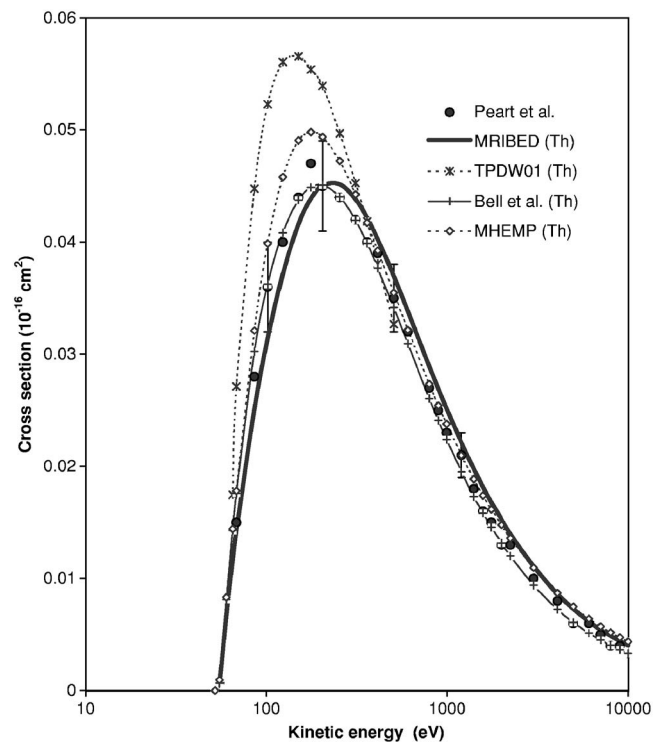


FIG. 7. Same as Fig. 6 for  $He^+$  with the experimental data now from Peart *et al.* [47].

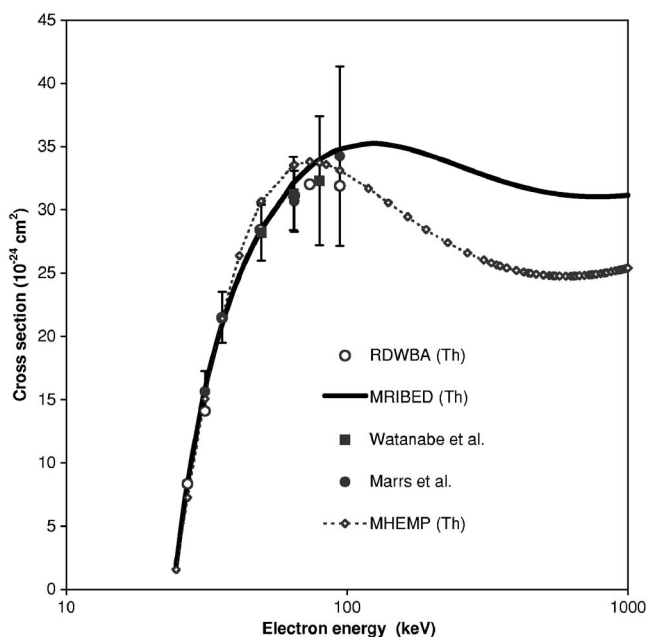


FIG. 8. Same as Fig. 5 for  $\text{Mo}^{41+}$  with experimental data in solid circles and solid rectangles from [48,49], respectively. The RDWBA results of [32] are given as open circles.

quantal calculations. As evident in Figs. 6–10 the MRIBED model provides a satisfactory description of the experimental results for  $\text{H-U}^{91+}$  in the whole energy range and good agreement with the RDWBA and TPDW01 predictions, except for  $\text{H}$  and  $\text{He}^+$  where the latter results overestimate the experimental cross sections in the low-energy region. The MHEMP model gives reasonable fits to the data except the cases of  $\text{H}$  and  $\text{He}^+$ . The assessed data generated from the

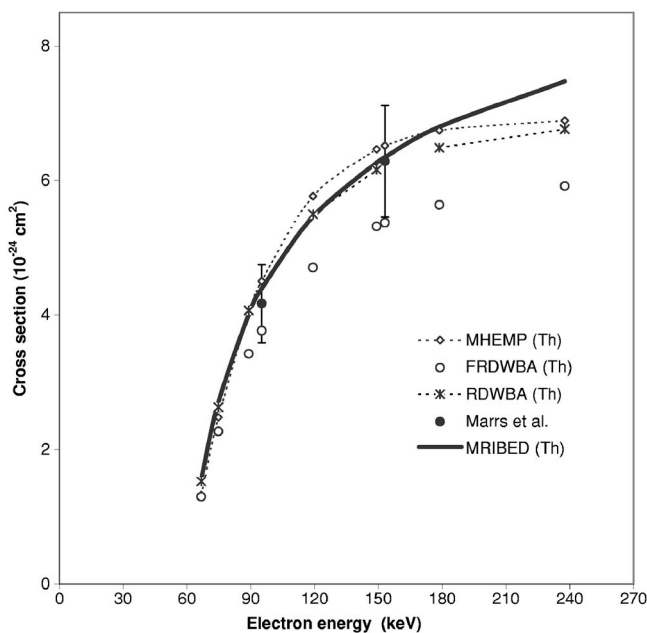


FIG. 9. Same as Fig. 6 for  $\text{Dy}^{65+}$  with the experimental data of [48] in solid circles. The RDWBA of [32] and FRDWBA of [36] and MHEMP [29] are shown as the dotted curve with asterisks, open circles, and dotted curve with asterisks, respectively.

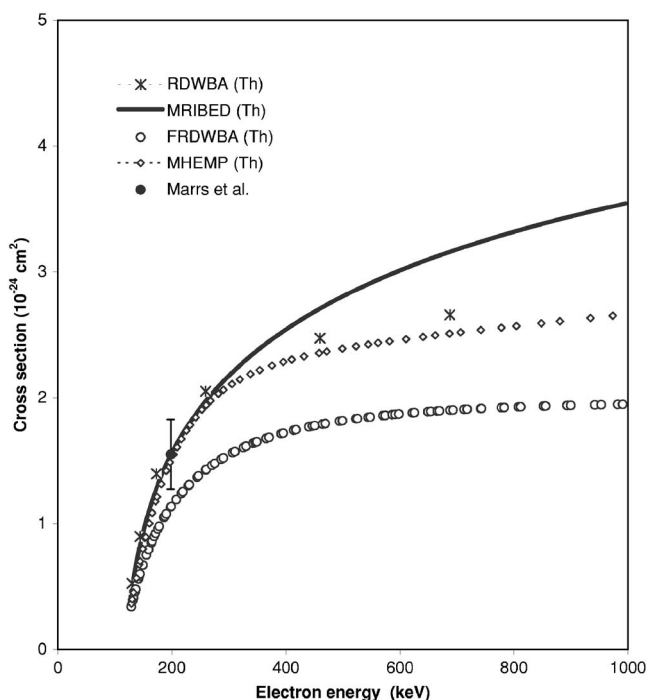


FIG. 10. Same as Fig. 6 for  $\text{U}^{91+}$  with the experimental data of [48] as solid circles, the RDWBA results of [32] as the dotted curve with asterisks, and FRDWBA predictions of [36] as open circles.

Bell's formula [37], with parameters being species dependent, are close to the experimental cross sections. The MRIBED model, with its simple structure, gives the best fit to the data in the overall assessment with all the targets in the H-like series. The TPDW01 and MHEMP results overestimate the experimental data for the cases of  $\text{H}$  and  $\text{He}^+$ . For  $\text{Dy}^{65+}$ , the MRIBED cross sections disagree with those calculated from the FRDWBA but agree closely with the RDWBA and MHEMP results. In the case of  $\text{U}^{91+}$ , the FRDWBA underestimates the experimental value as well as the predicted cross sections from the RDWBA theory and the MRIBED and MHEMP models. The MRIBED model disagrees with MHEMP for  $\text{Mo}^{41+}$  (Fig. 8) and with both RDWBA and MHEMP for  $\text{U}^{91+}$  (Fig. 10) in predicting the cross sections at higher energies.

In Figs. 11–14 comparisons are made of the MRIBED predictions for the  $\text{Li}$ ,  $\text{N}^{4+}$ ,  $\text{Ti}^{19+}$ ,  $\text{V}^{20+}$ ,  $\text{Cr}^{21+}$ ,  $\text{Mn}^{22+}$ ,  $\text{Fe}^{23+}$ , and  $\text{U}^{89+}$  targets in the Li isoelectronic sequence, with the experimental data from Zapesochnyl and Aleksakhin [51], McFarland and Kinney [52], Jalin *et al.* [53], Crandall *et al.* [54,55], Donets and Ovsyannikov [45], and Rester and Dance [57]. The theoretical calculations, compared with the MRIBED results for the Li-like systems, are CCC of Bray [33], CB of Jacobowicz and Moores [35], DWBA of Wong *et al.* [56], and the model predictions from BRY [9]. As apparent from Fig. 11, although the MRIBED predictions for Li show discrepancies with the experimental data, it seems to perform better than the CCC calculations [33]. The calculated peak position from MRIBED is shifted towards the higher energies relative to those resulting from both the BRY and Bell predictions, which are close to each other. Figure 12 shows that the MRIBED model produces a satisfactory fit to the experimental data of  $\text{N}^{4+}$ .

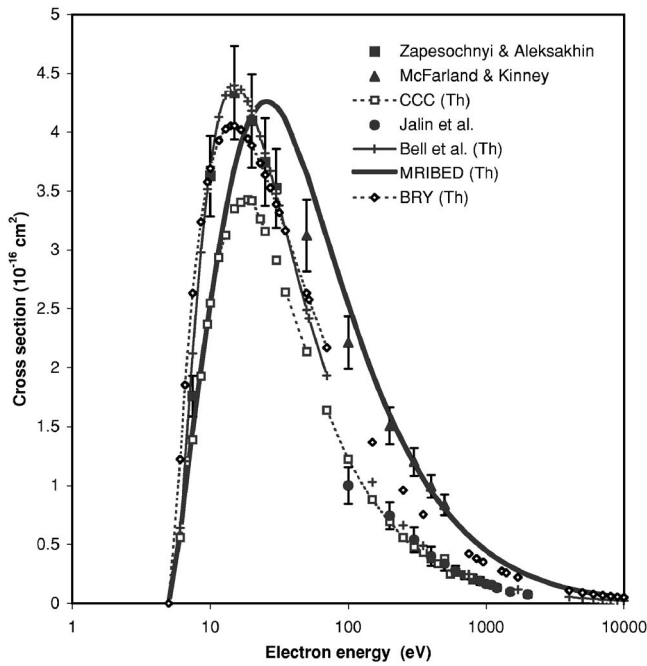


FIG. 11. Same as Fig. 6 for Li with the experimental data as solid circles, solid triangles, and solid rectangles from [51–53], respectively. The dotted curve with open rectangles and those with open diamonds represent, respectively, the BRY [9] and the CCC calculations of [33].

Figure 13 compares the calculated  $2s$ -orbit ionization cross sections for  $U^{89+}$  from the present MRIBED model with the RDWBA results of [32]. The MRIBED cross sections are determined by the ionization potential  $I$  and kinetic energy  $U$  of the bound electron in addition to the incident energy. The  $I(1s)=29.38$  keV and  $U(1s)=33.31$  keV values for the  $K$ -shell ionization of Sn are close to the  $I(2s)=32.90$  keV and  $U(2s)=27.87$  keV for the  $2s$  orbit of  $U^{89+}$  and, in consequence, the EI cross sections for the latter are expected to be very similar to the half (considering one electron in the  $2s$  orbit of  $U^{89+}$ ) of the  $K$ -shell ionization cross sections for Sn. The MRIBED results agree very well with the experimental cross sections (reduced by a factor of 0.5) for Sn from Rester and Dance [57]. The RDWBA and MRIBED results are close to each other up to about 100 keV, and beyond that the former decrease more rapidly in contradiction to the experimental cross sections.

In Fig. 14, the MRIBED predictions for  $Ti^{19+}$ ,  $V^{20+}$ ,  $Cr^{21+}$ ,  $Mn^{22+}$ , and  $Fe^{23+}$ , at the incident energy approximately 2.3 times the respective threshold energy, are compared with the experimental EI cross sections and DWBA calculations of Wong *et al.* [56] as well as the BRY [9] results. The DWBA calculations have been done using the code of [31]. The agreement among the MRIBED predictions, the experimental data, and the DWBA and BRY results is excellent.

**IV. CONCLUSIONS**

The MRIBED model is seen to provide a good description of the experimental EI cross-section data for hydrogen and

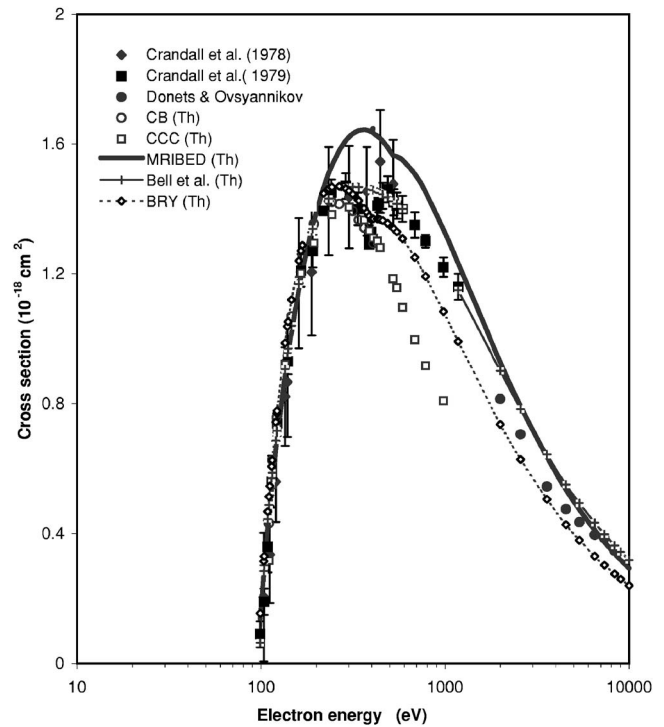


FIG. 12. Same as Fig. 11 for  $N^{4+}$  with the experimental data as open circles, solid rectangles, and solid diamonds of [45,54,55], respectively. The CB results of [35] are shown as open circles.

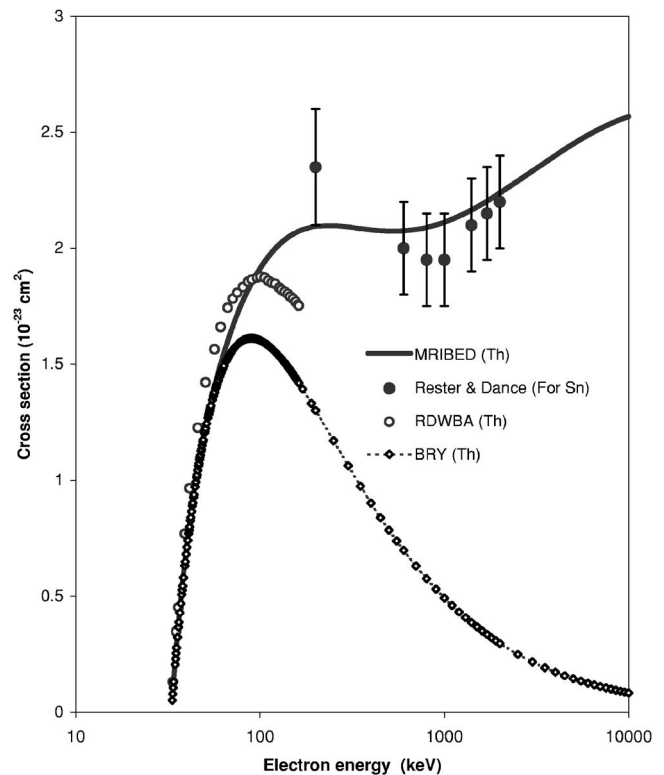


FIG. 13. EI ionization cross sections of  $U^{89+}$  for the  $2s$  orbit. The present MRIBED calculations and the RDWBA results of [32] are compared with the reduced values of the experimental data [57] of the  $K$ -shell ionization of Sn (see text for explanation).

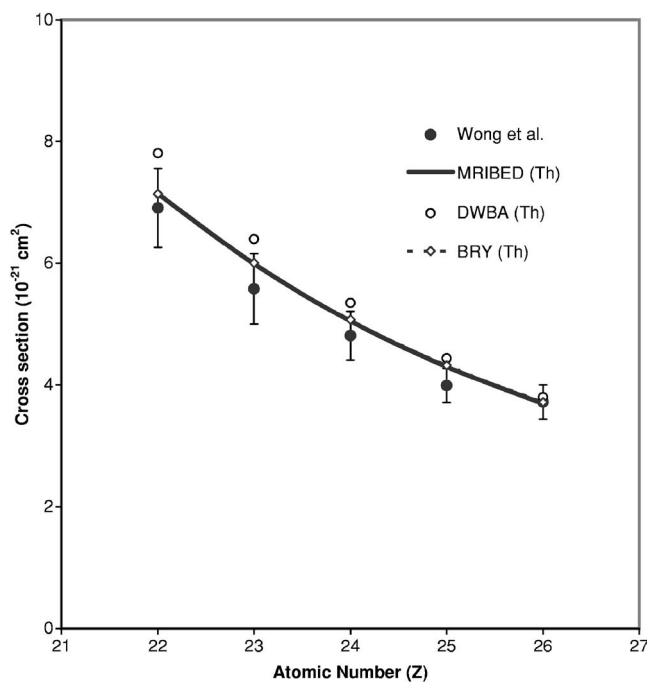


FIG. 14. The EI ionization cross sections of  $Ti^{19+}$ ,  $V^{20+}$ ,  $Cr^{21+}$ ,  $Mn^{22+}$ , and  $Fe^{23+}$  at the incident energy of approximately 2.3 times the threshold. The experimental data and the DWBA results are from [56]. The present MRIBED predictions are shown as the solid curve.

lithium isoelectronic series except for the lone case of atomic Li. The description has been accomplished for 16 targets in the range  $Z=1-92$  using a single set of parameters  $m=0.365$  and  $n=0.050$ . In the case of Li, the overall perfor-

mance of the MRIBED model is comparable to other theoretical calculations (Fig. 10). In some of the species—e.g., H (Fig. 5) and  $U^{89+}$  (Fig. 13)—the MRIBED model works better than other theories considered herein.

The success of the MRIBED model, in the present study, in the description of the EI ionization for targets in the H and Li isoelectronic sequences coupled with that achieved with the MRIBED model on members of He [24] and Be [27] isoelectronic series as well as on the  $K$ -shell ionization of atoms [26] indicates that the parameters  $d_1$  and  $d_2$ , which are dependent on the electronic structure of the targets, play a pivotal role. The values  $d_1=d_2=0.0$  are seemingly locked to the cases of ionization from an  $s$  orbit. The form of  $F(Z)$  for a filled  $s$  orbit is  $F(Z)=1$ , and the MRIBED model reduces to the MRIBED one of [26,27].

The MRIBED model, in its performance to describe the EI ionization of the H- and Li-like species, is seen to be comparable to and even better, in some cases, than sophisticated theories like the DWBA, CB, RDWBA, and CCC. It is demonstrated that the present MRIBED model produces very encouraging and reliable results for ionization from any filled and unfilled  $s$ -orbital targets. In order to decide the predictive role of our method, it is our intention to extend this model to other open-subshell targets, especially the  $p$ -orbital target, since the open-subshell systems remain a challenge. The MRIBED model with its simple structure may turn out to be a very lucrative alternative for generating accurate data for plasma modeling codes.

#### ACKNOWLEDGMENT

Authors wish to thank Professor F. Bary Malik, Southern Illinois University, Carbondale, IL, USA for his encouragement.

- [1] S. M. Younger and T. D. Märk, in *Electron Impact Ionization*, edited by T. D. Märk, G. H. Dunn (Springer-Verlag, Berlin, 1985), p. 24.
- [2] D. L. Moores and K. J. Reed, *Adv. At., Mol., Opt. Phys.* **34**, 301 (1994).
- [3] I. E. McCarthy and E. Wegold, *Phys. Rep., Phys. Lett.* **27C**, 275 (1976).
- [4] H. Tawara and T. Kato, *At. Data Nucl. Data Tables* **36**, 167 (1987).
- [5] J. J. Thomson, *Philos. Mag.* **23**, 449 (1912).
- [6] W. Lotz, *Z. Phys.* **216**, 241 (1968).
- [7] W. Lotz, *Z. Phys.* **232**, 101 (1970).
- [8] M. Gryzinski, *Phys. Rev.* **138**, 336 (1965).
- [9] V. A. Bernshtam, Y. V. Ralchenko, and Y. Maron, *J. Phys. B* **33**, 5025 (2000).
- [10] H. Deutsch and T. D. Märk, *Int. J. Mass Spectrom. Ion Process.* **79**, R1 (1987).
- [11] H. Deutsch, K. Becker, S. Matt, and T. D. Märk, *Int. J. Mass Spectrom.* **197**, 37 (2000).
- [12] D. Margreiter, H. Deutsch, and T. D. Märk, *Int. J. Mass Spectrom. Ion Process.* **139**, 127 (1994).
- [13] H. Deutsch, K. Becker, and T. D. Märk, *Contrib. Plasma Phys.* **35**, 421 (1995).
- [14] H. Deutsch, K. Becker, and T. D. Märk, *Int. J. Mass Spectrom.* **177**, 47 (1998).
- [15] H. Deutsch, K. Becker, and T. D. Märk, *Int. J. Mass Spectrom.* **185**, 319 (1999).
- [16] H. Deutsch, K. Becker, P. Defrance, U. Onthong, R. Parajuli, M. Probst, S. Matt, and T. D. Märk, *J. Phys. B* **35**, L65 (2002).
- [17] H. Deutsch, K. Becker, B. Gstir, and T. D. Märk, *Int. J. Mass Spectrom.* **213**, 5 (2002).
- [18] Y.-K. Kim and M. E. Rudd, *Phys. Rev. A* **50**, 3954 (1994).
- [19] W. Hwang, Y.-K. Kim, and M. E. Rudd, *J. Chem. Phys.* **104**, 2956 (1996).
- [20] Y.-K. Kim, W. Hwang, N. M. Weinberger, M. A. Ali, and M. E. Rudd, *J. Chem. Phys.* **106**, 1026 (1997).
- [21] Y.-K. Kim, J. Migdalek, W. Siegel, and J. Bieron, *Phys. Rev. A* **57**, 246 (1998).
- [22] Y.-K. Kim and P. M. Stone, *Phys. Rev. A* **64**, 052707 (2001).
- [23] K. K. Irikura and Y.-K. Kim, *J. Res. Natl. Inst. Stand. Technol.* **107**, 63 (2002).
- [24] M. A. Uddin, M. A. K. Fazlul Haque, A. K. Basak, and B. C. Saha, *Phys. Rev. A* **70**, 032706 (2004).
- [25] W. M. Huo, *Phys. Rev. A* **64**, 042719 (2001).



- [26] M. A. Uddin, A. K. F. Haque, M. M. Billah, A. K. Basak, K. R. Karim, and B. C. Saha, *Phys. Rev. A* **71**, 032715 (2005).
- [27] M. A. Uddin, A. K. F. Haque, M. S. Mahbub, K. R. Karim, A. K. Basak, and B. C. Saha, *Int. J. Mass. Spectrom.* **244**, 76 (2005).
- [28] C. J. Fontes, D. H. Sampson, and H. L. Zhang, *Phys. Rev. A* **59**, 1329 (1999).
- [29] M. A. Uddin, A. K. F. Haque, K. R. Karim, and A. K. Basak, *Phys. Scr.* (to be published).
- [30] S. M. Younger, *J. Quant. Spectrosc. Radiat. Transf.* **26**, 329 (1981).
- [31] H. L. Zhang and D. H. Sampson, *Phys. Rev. A* **42**, 5378 (1990).
- [32] D. L. Moores and K. J. Reed, *Phys. Rev. A* **51**, R9 (1995).
- [33] I. Bray, *J. Phys. B* **28**, L247 (1995).
- [34] T.-Y. Kuo and K.-N. Huang, *Phys. Rev. A* **64**, 032710 (2001).
- [35] H. Jacobowicz and D. L. Moores, *J. Phys. B* **14**, 3733 (1981).
- [36] C. J. Fontes, D. H. Sampson, and H. L. Zhang, *Phys. Rev. A* **48**, 1975 (1993).
- [37] K. L. Bell, H. B. Gilbody, J. G. Hughes, A. E. Kingston, and F. J. Smith, *J. Phys. Chem. Ref. Data* **12**, 891 (1983).
- [38] M. Inokuti, *Rev. Mod. Phys.* **43**, 297 (1971).
- [39] J. P. Desclaux, *At. Data Nucl. Data Tables* **12**, 325 (1973).
- [40] M. Y. Amusia and L. V. Chernysheva, *Computations of Atomic Processes* (Institute of Physics, Bristol, 1997).
- [41] F. Scheid, *Numerical Analysis*, Schaums Outline Series (McGraw-Hill, Singapore, 1988).
- [42] M. B. Shah, D. S. Elliot, and H. B. Gilbody, *J. Phys. B* **20**, 3501 (1987).
- [43] R. Rejoub, B. G. Lindsay, and R. F. Stebbings, *Phys. Rev. A* **65**, 042713 (2002).
- [44] M. Duponchelle, M. Khoulid, E. M. Onalim, H. Zhany, and P. Defrance, *J. Phys. B* **30**, 729 (1997).
- [45] E. D. Donets and V. P. Ovsyannikov, *Sov. Phys. JETP* **53**, 466 (1981).
- [46] R. E. Marrs, S. R. Elliott, and D. A. Knapp, *Phys. Rev. Lett.* **72**, 4082 (1994).
- [47] B. Peart, D. S. Walton, and K. T. Dolder, *J. Phys. B* **2**, 1347 (1969).
- [48] R. E. Marrs, S. R. Elliott, and J. H. Scofield, *Phys. Rev. A* **56**, 1338 (1997).
- [49] H. Watanabe, F. J. Currell, H. Kuramoto, S. Ohtani, B. E. O'Rourke, and X. M. Tong, *J. Phys. B* **35**, 5095 (2002).
- [50] C. Møller, *Z. Phys.* **70**, 786 (1931).
- [51] I. P. Zapesochnyl and I. S. Aleksakhin, *Sov. Phys. JETP* **28**, 41 (1969).
- [52] R. H. McFarland and J. D. Kinney, *Phys. Rev.* **137**, A1058 (1965).
- [53] R. Jalin, R. Hagemann, and R. Botter, *J. Chem. Phys.* **59**, 952 (1973).
- [54] D. H. Crandall, R. A. Phaneuf, B. E. Hasselquist, and D. C. Gregory, *J. Phys. B* **12**, L249 (1979).
- [55] D. H. Crandall, R. A. Phaneuf, and P. O. Taylor, *Phys. Rev. A* **18**, 1911 (1978).
- [56] K. L. Wong, P. Beiersdorfer, M. H. Chen, R. E. Marrs, K. J. Reed, J. H. Scofield, D. A. Vogel, and R. Zasadzinski, *Phys. Rev. A* **48**, 2850 (1993).
- [57] D. H. Rester and W. E. Dance, *Phys. Rev.* **152**, 1 (1966).